MATHEMATICAL MODEL OF A MOTION CUEING ALGORITHM FOR 6DOF FLIGHT SIMULATOR

Alina-Ioana CHIRA[1], Constantin OLIVOTTO[2], Ion STROE[3]

The present paper proposes the development of a motion cueing algorithm for a flight simulator based on a serial robot motion platform using genetic algorithms for the optimization of the optimal washout filter based on linear quadric regulator. The design, implementation and testing of the algorithm were performed using the dynamic simulation system for pilot-in-the-loop applications, called RoFSim. The proposed motion cueing algorithm converts aircraft dynamics into robot movements, generating high-fidelity motion within the physical limits of the flight simulator. This reproduction includes specific forces and accelerations, allowing the simulation to replicate sensations similar to those experienced in a real aircraft.

The results obtained demonstrate the stability and performance of the implemented optimal washout filter, highlighting the potential use of the proposed algorithm in R&D projects and its further development.

Keywords: flight simulator, motion cueing algorithm, serial robot, optimal washout filter, LQR, genetic algorithm

1. Introduction

The objective of this research is based on the problem of solving how to transmit motion cues in a six-degree-of-freedom (6DoF) flight simulator (Figure 1) using a motion cueing algorithm, also known to as a washout filter algorithm.

The washout filter (WF) is an algorithm that aims to provide the pilot with the acceleration sensations that would be experienced in a real aircraft on a motion platform with a severely restricted workspace ([1], [2], [3]). It receives as input data the linear accelerations and angular velocities of the simulated aircraft and provides as output data the trajectory to be followed by the end-effector of the motion platform in Cartesian coordinate system. This algorithm consists of a combination of three channels - rotational, translational, tilt coordination - each of which is composed of low-pass or high-pass filters, depending on the behaviour

[1] Eng., National Institute for Aerospace Research "Elie Carafoli" – INCAS Bucharest, Romania, e-mail: chira.alina@incas.ro (corresponding author)

[2] PhD Eng., National Institute for Aerospace Research "Elie Carafoli" – INCAS Bucharest, Romania, e-mail: olivotto.constantin@incas.ro

[3] Prof., Department of Mechanics, University POLITEHNICA București, Romania, e-mail: ion.stroe@gmail.com

that the flight simulator is intended to represent. The main benefit of this washout filter is to provide motion cues that ensure human perception [4].

Fig. 1 Dynamic simulation system for pilot-in-the-loop applications – 6DoF flight simulator RoFSim

In addition, the motion produced must be within the limits and constraints of the proposed flight simulator platform [5]. The main theories in this area are the optimal ([6], [7], [8], [9], [10]), adaptive ([3], [9], [11], [12], [13], [14]) and robust ([6], [8], [9], [15], [16], [17]) washout filters.

In the paper [2] the authors described a simulator design problem and presented a new method based on the human vestibular system. This optimal washout filter (OWF) algorithm was based on human motion perception and considered the vestibular system ([19], [20]). The vestibular system is located in the inner ear and consists of semicircular canals and otolith organs for detecting rotational and linear motion. Essentially, the method integrated a mathematical model of the human vestibular system to minimise the error of perception between the pilot in the simulator and the pilot in a real aircraft cockpit. The method used a quadratic linear regulator based (LQR) on optimal control techniques to develop higher order filters prior to real-time application, and designed a cost function that depends on both the real and simulated aircraft pilot's perception error and platform motion. In developing an optimal washout filter based on the LQR method, the key problem is to find a suitable matrix of transfer functions $W(s)$. This matrix relates simulator and aircraft motion inputs in an attempt to minimise the cost function by limiting both the sensing error between the simulator and aircraft pilot and the platform motion.

2. Mathematical model of the optimal washout filter

The washout filter is a motion algorithm that converts the acceleration and angular velocity of a simulated vehicle into the motion of the simulator platform. The motion produced must be within the limits and constraints of the motion platform used for the flight simulator.

The optimal washout filter was first developed by Sivan and co-workers [2] with four assumptions: (a) the vestibular system dominates the perception of motion cues in a flight simulator; (b) the discrepancy between motion cues in the real aircraft and in the motion simulator can be measured by the root mean square value of the vestibular error; (c) real aircraft motion can be modelled as a random process independent of motion platform constraints; and (d) dynamic systems, including vestibular systems, can be represented by linearized equations.

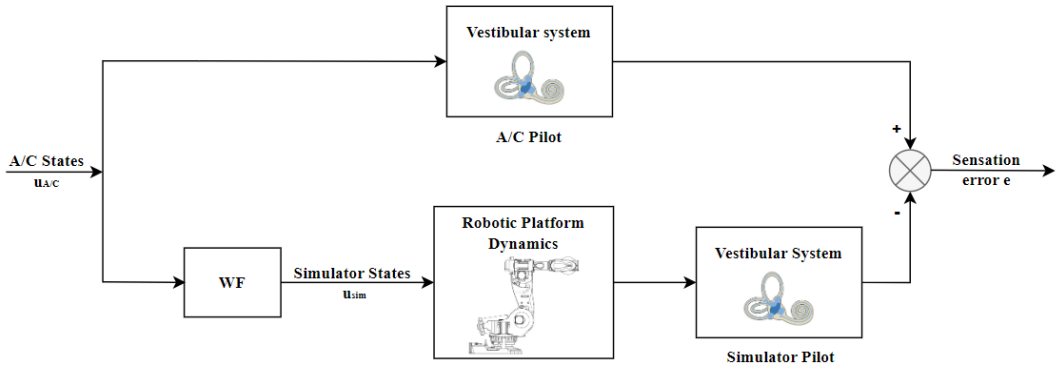

Fig. 2 Structure of the optimal control washout filter algorithm based on LQR, adaptation [11]

The schematic diagram of the optimal washout filter based on LQR shown in Figure 2 includes two separate channels that generate the perception of motion between the real aircraft and the flight simulator. In both channels, the vestibular system represents the pilot's vestibular system.

The goal of the optimal washout filter based on LQR (Figure 3) is to determine the transfer function $W(s)$ that relates the flight simulator motion input (u_{sim}) to the aircraft motion input ($u_{A/C}$).

$$u_{sim}(s) = W(s) \cdot u_{A/C}(s) \tag{1}$$

Control inputs, including accelerations and Euler angles, are used to generate the basic commands for the desired motion. Thus the optimal washout filter algorithm determines the simulator acceleration by minimising the human feel error between the simulator and the aircraft, as well as the linear and angular motion of the platform. The objective of the algorithm is therefore to limit the human

perception error and platform motion within the physical workspace of the robotic platform.

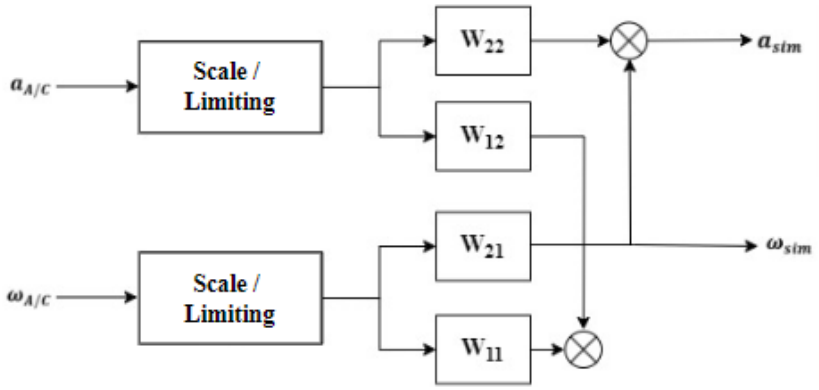

Fig. 3 Optimal washout filter algorithm, adaptation [6]

The objective function of the motion algorithm includes the perception error and constraints related to the motion in the workspace of the flight simulator motion platform, where $a_{A/C}$ and a_{sim} represent the detected acceleration at the actual position and at the workspace position. Also, $\omega_{A/C}$ and ω_{sim} are the rotational velocities detected at these positions. Due to the use of a model with two inputs and two outputs, four transfer functions (W_{11}, W_{21}, W_{12} and W_{22}) are used, each representing the effect of each input on each output. Input u is represented as follows:

$$u = \begin{bmatrix} u_1 \\ u_2 \end{bmatrix} = \begin{bmatrix} \dot{\theta} \\ a_{Ax} \end{bmatrix} \tag{2}$$

An important step in the implementation of the algorithm is how the definition of the tilt coordination effect is. The tilt coordination aims to calculate the low frequency components on the horizontal axis, X direction, and on the lateral axis, Y direction, while the low frequency components on the vertical axis, Z direction, are not calculated. Figure 4 shows how the tilt coordination is formulated to generate acceleration on the horizontal and lateral axes.

The specific surge force in the centre motion of the simulator can be obtained as follows, but considering the approximation for small angles, $\sin(\theta_t)$ and $\cos(\theta_t)$ can be replaced by θ_t and 1 respectively:

$$f_s = a_{Ax} \cdot \cos(\theta_t) + g \cdot \sin(\theta_t) \cong a_{Ax} + g \cdot \theta_t \tag{3}$$

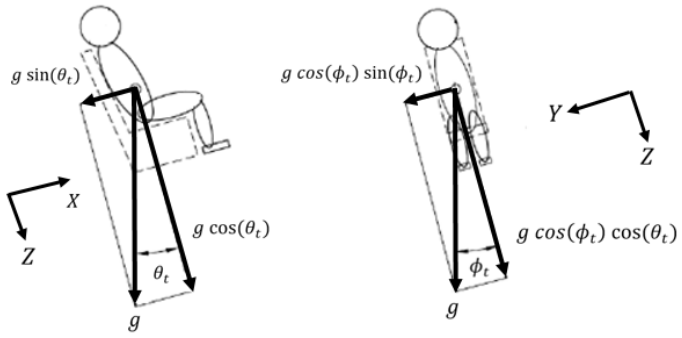

Fig. 4 Formulation and effect of the tilt coordination

The specific detected value a_{Ax_s} is related to the specific stimulus strength detected by the otolith model and is entered into the equation below as follows:

$$a_{Ax\_s} = k_O \frac{s+A_0}{(s+B_0)(s+B_1)} \cdot f_s \tag{4}$$

By applying the Laplace transform, a new form of the equation can be obtained. The term $\frac{1}{s}$ is the integration of the angular velocity.

$$f_s(s) = a_{Ax}(s) + g \cdot \frac{1}{s} \cdot \dot{\theta}(s) \tag{5}$$

Substituting equation (3) into equation (2) gives the following equation:

$$a_{Ax\_s} = k_O \frac{s+A_0}{(s+B_0)(s+B_1)} \left(a_x(s) + g \cdot \frac{1}{s} \cdot \dot{\theta}(s) \right) \tag{6}$$

where A_0, B_0 and $B_1$are the specific parameters of the otolith model.
The sensed angular velocity $\dot{\theta}_s$ is related to the actual angular velocity sensed by the semicircular canal. Semicircular canals can detect the sensation of rotational motion. Telban and Cardullo [18] proposed a transfer function of the semicircular channels model to detect angular velocity sensation when applied as a stimulus. This transfer function includes the torsional pendulum model [19], the adaptation operator and a lead term. This function provides the best approximation to the true dynamics of the vestibular sensory system for rotational motion. The semicircular canal model is defined as follows:

$$\dot{\theta}_s = \frac{k_{sc} \cdot \tau_1 \cdot \tau_a \cdot s^2 (1+\tau_L \cdot s)}{(\tau_1 \cdot s+1)+(\tau_2 \cdot s+1)+(\tau_a \cdot s+1)} \dot{\theta} \tag{7}$$

where τ_1, τ_2, τ_L and τ_a are the long time constant, short time constant, lead term and adaptation operator constant, respectively.

3. Scaling and limiting

The simulator's motion platform has physical limits, so its dynamics must be constrained within these limits and constraints. Therefore, within the working scheme of the motion algorithm, a constraint has been applied to the translational and rotational channels, and at the same time, a scaling has been applied to the model input signals.

Limiting and scaling apply to both the aircraft translational input signals $\boldsymbol{a_{A/C}}$and the rotational input signals $\boldsymbol{\omega_{A/C}}$. Limiting and scaling change the amplitude of the input signal uniformly across all frequencies. Limiting is a non-linear process that reduces the signal so that it is limited to a value less than a certain amplitude. Limiting and scaling can be used to reduce the motion response of a flight simulator. A third-order polynomial was used for scaling and was implemented in the general scheme of the motion algorithm. When the magnitude of the input to the simulator motion system is small, it is desired that the amplitude be relatively high, otherwise the output will be below the pilot's perception threshold. And when the input magnitude is high, it is desired that the amplitude is relatively small to avoid the case where the simulator attempting to exceed the hardware limits.

For the implementation of the procedure, the input was denoted by $\boldsymbol{x_a}$, and the output by $\boldsymbol{x_z}$. Then $\boldsymbol{x_{amax}}$ was defined as the desired maximum input and $\boldsymbol{x_{zmax}}$ as the maximum output, and $\boldsymbol{s_0}$ and $\boldsymbol{s_1}$ the slopes at $\boldsymbol{x_a = 0}$ and $\boldsymbol{x_a = x_{amax}}$ respectively. Four desired non-linear scaling characteristics are defined as follows:

$$\begin{gathered} x_a = 0 \Longrightarrow x_z = 0 \\ x_a = x_{amax} \Longrightarrow x_z = x_{zmax} \\ x_z'|_{x_a=0} = s_0 \\ \boldsymbol{x_z'|_{x_a=x_{amax}} = s_1} \end{gathered} \tag{8}$$

The third-order polynomial scaling used to provide functions with desired characteristics is of the form:

$$\boldsymbol{x_z = p_3 x_a^3 + p_2 x_a^2 + p_1 x_a^1 + p_0} \tag{9}$$

where

$$\begin{gathered} p_0 = 0 \\ p_1 = s_0 \\ p_2 = x_{amax}^{-2}(3 \cdot x_{zmax} - 2 \cdot s_0 \cdot x_{amax} - s_1 \cdot x_{amax}) \\ \boldsymbol{p_3 = x_{amax}^{-3}(s_0 \cdot x_{amax} - 2 \cdot x_{zmax} + s_1 \cdot x_{amax})} \end{gathered} \tag{10}$$

Parameter scaling for the translational motion:

$$\boldsymbol{max|x_{amax}| = 6\ m/s^2}$$

$$\boldsymbol{max|x_{zmax}| = 6\frac{m}{s^2}}\ \text{for}\ \boldsymbol{X}$$

$$\boldsymbol{max|x_{zmax}| = 0.8\frac{m}{s^2}}\ \text{for}\ \boldsymbol{Y}\ \text{and}\ \boldsymbol{Z} \tag{11}$$

and the coefficients are:

$$\begin{gathered} s_0 = 1 \text{ for } X \\ s_0 = 0.2 \text{ for } Y \text{ and } Z \\ s_1 = 0.1 \text{ for } X, Y \text{ and } Z \end{gathered} \tag{12}$$

Parameter scaling for the rotational motion:

$$max|x_{amax}| = 3.14\ \frac{rad}{s}$$

$$\boldsymbol{max|x_{zmax}| = 1.57\ \frac{rad}{s}} \tag{13}$$

and the coefficients are:

$$\begin{gathered} s_0 = 0.785 \text{ for } X, Y \text{ and } Z \\ s_1 = 0.1 \text{ for } X, Y \text{ and } Z \end{gathered} \tag{14}$$

The linear accelerations on all axes are limited to $\boldsymbol{6\frac{m}{s^2}}$ for the translational channel, and the limit for the rotational channel is $\boldsymbol{3.14\frac{rad}{s}}$. An example of this polynomial gain is shown in the Fig. 5.

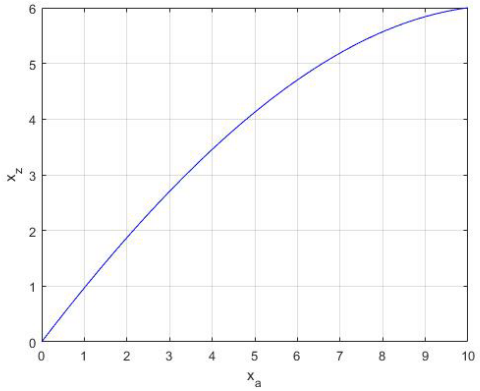

Fig. 5 Nonlinear scaling

4. Methods and materials

The structure of the aircraft simulation system for the robotic platform-based motion system [20] is shown in Figure 6.

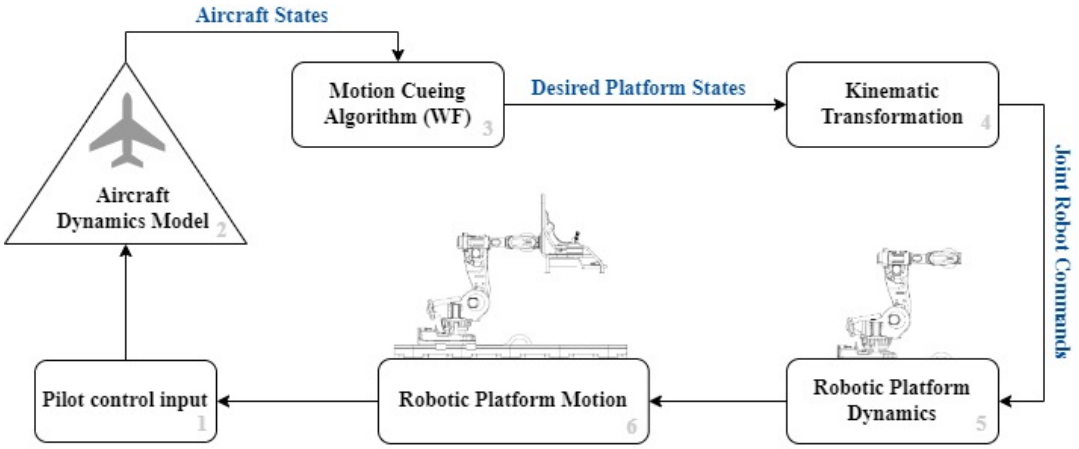

Fig. 6 High level architecture for 6DoF flight simulator RoFSim

Inputs from by the operator (pilot) are passed to the aircraft dynamics model, generating the aircraft state vector. Passing the aircraft state vector through the motion algorithm produces the desired motion cues and the robot platform states that provide the motion to the simulator. The desired robot platform states are then transformed from the degrees of freedom space to the axis workspace, generating commands to the six robot axes. The axis motion commands act as inputs to the robot platform, resulting in the actual motion of the simulator. The operator (pilot) inputs are transferred to the dynamic simulation model running on a real-time platform. The operator (pilot) signals can come from various specific control devices such as flap position, rudder actuation, throttle actuation, etc. The outputs from the dynamic aircraft model are measured in terms of translational accelerations, rotational angles and angular velocities; outputs that are required to reproduce the motion feedback to the simulator. The aim is to induce realistic motion in the simulation cabin. Obviously, due to the limitations of the simulator workspace, the motion cannot be identical to that of the aircraft and must be compressed. This feature is provided by motion detection algorithms as shown in Figure 2. After determining the position and orientation of the cabin, the individual command input from the six-degree-of-freedom robot is calculated from the inverse kinematics transformation. The resulting command inputs are passed through the collision prevention filter and are sent to the robot. This step closes the motion feedback loop for the test pilot.

In the implementation procedure of the optimal washout filter based motion cueing algorithm, the input signal vector is taken as:

$$u_{A/C}(s) = \left[a_{Ax}(s) \;\; \dot{\theta}(s)\right] \tag{15}$$

By completing the equations and deriving the new terms, a generalised transfer function is generated that links the real motion of the aircraft to the motion of the flight simulator.

$$u_{sim}(s) = W(s) \cdot u_{A/C}(s) \tag{16}$$

where $\boldsymbol{W}$ is the matrix of the optimised transfer function that transfers the simulator inputs $\boldsymbol{u_{sim}(s)}$ to the real motion $\boldsymbol{u_{A/C}(s)}$. The transfer function W(s) is defined in matrix form as follows:

$$W(s) = \begin{bmatrix} W_{11} & W_{12} \\ W_{21} & W_{22} \end{bmatrix} \tag{17}$$

The form of each transfer function W_{ij} is shown in equation (18), in total twelve parameters are used to complete the denominator and numerator respectively. The denominator parameters are unique for each W_{ij}.

$$W_{ij} = \frac{a_5 \cdot s^5 + a_4 \cdot s^4 + a_3 \cdot s^3 + a_2 \cdot s^2 + a_1 \cdot s + a_0}{b_5 \cdot s^5 + b_4 \cdot s^4 + b_3 \cdot s^3 + b_2 \cdot s^2 + b_1 \cdot s + b_0} \tag{18}$$

Finding the appropriate matrix for the numerical solution is not straightforward and can lead to failure, so the genetic algorithm was used to identify the optimal parameters.

The objective function for this problem is shown in the equation below as follows:

$$F_c = \int_0^{t_f} \left[|z_{sim} - z_0| + \left|p_{A/C} - p_{sim}\right|\right] dt \tag{19}$$

The lift position of the flight simulator is denoted by z_{sim} and the base value, the physical constraint of the flight simulator, is denoted by z_0. And $p_{A/C}$ is a function of the sensed perception (human perception) before and after applying the wash filter. The notation A/C and sim denote the actual motion and the motion of the simulator, respectively. The last time in the equation is defined by t_f.

The aim of the method is to limit the error of human perception and platform movement according to the working space limitations of the motion platform - serial robotic system. Evolutionary algorithms are robust methods for finding near-optimal solutions with the ability to handle undefined evaluations that have certain properties, such as: coupling; time variation; discontinuity; noise; and probability [21]. Genetic algorithm is one of the efficient evolutionary algorithms that has wide applications [22]. It is a heuristic, robust and reliable search method that generates a solution through a process that mimics natural selection and evolution.

The genetic algorithm is robust and efficient in exploring the search space to identify optimal solutions. Each solution in its generation is represented by a chromosome made up of genes:

$$A_c^i = \left[A_{c,1}^i, A_{c,2}^i, \dots, A_{c,n}^i\right] \tag{20}$$

where c is the number of chromosomes in the population and n is the number of genes in each chromosome. To evaluate each individual, it is necessary to establish a defined performance index. The objective function is formulated to rank the performance of each individual [23]. For the proposed method, the overall objective function consists of five sub-problems as follows:

I. Minimisation of translational and rotational errors of human perception between what pilots feel in the real aircraft and in the simulator.
II. Minimise the angular and linear displacements of the motion platform to operate within its physical limits.
III. Minimise the variation of perception errors.
IV. Maximising the correlation coefficient, defined as the Pearson moment correlation coefficient, to increase the traceability of the reference signal shape in the produced signal.
V. Minimise the acceleration and velocity of the moving platform due to physical constraints.

Therefore, the objective function at each i iteration for the c individual is defined as the sum of the sub-objective functions:

$$O(A_c^i) = O_{c\_sener}^i + O_{c\_cor}^i + O_{c\_lim}^i \tag{21}$$

where $O_{c\_sener}^i$ is an objective function related to the total error of human perception, $O_{c\_cor}^i$ is an objective function of the correlation coefficient, and $O_{c\_lim}^i$ is an objective limiting function.

The present algorithm also takes into account the effects of non-linearities, taking into account factors such as: tilt coordination (human threshold limiter), which affects human perception, physical constraints of the motion platform and the correlation coefficient. The chromosomes in the genetic algorithm are initialised using the individuals obtained from the results of the optimal washout filter algorithm.

5. Results

This chapter presents specific results for the optimal washout filter algorithm that was formulated, designed, developed, implemented and tested to improve the flight simulation environment using the IRB 7600-500 serial robot system as the motion platform for the RoFSim flight simulator. The vestibular system parameters for the otolith and semicircular canals are shown in the following tables according to [18]. Table 1 shows the specific force parameters for the otolith system and the frequency response of the specific force sensation transfer function for the otolith system is shown in Figure 7.

Table 1

Specific force parameters for the otolith system [24]

	X	**Y**	**Z**
$\boldsymbol{k_{ot}}$	0.4	0.4	0.4
$\boldsymbol{\tau_1}$ $[s]$	5	5	5
$\boldsymbol{\tau_2}$ $[s]$	0.016	0.016	0.016
$\boldsymbol{\tau_L}$ $[s]$	10	10	10
$\boldsymbol{A_0}$ $[s^{-1}]$	$1/\tau_L$	$1/\tau_L$	$1/\tau_L$
$\boldsymbol{B_0}$ $[s^{-1}]$	$1/\tau_1$	$1/\tau_1$	$1/\tau_1$
$\boldsymbol{B_1}$ $[s^{-1}]$	$1/\tau_2$	$1/\tau_2$	$1/\tau_2$
$\boldsymbol{k_0}$	$k_{ot}\tau_1\tau_2/\tau_L$	$k_{ot}\tau_1\tau_2/\tau_L$	$k_{ot}\tau_1\tau_2/\tau_L$
$\boldsymbol{dTH}$ $[m/s^2]$	0.17	0.17	0.28

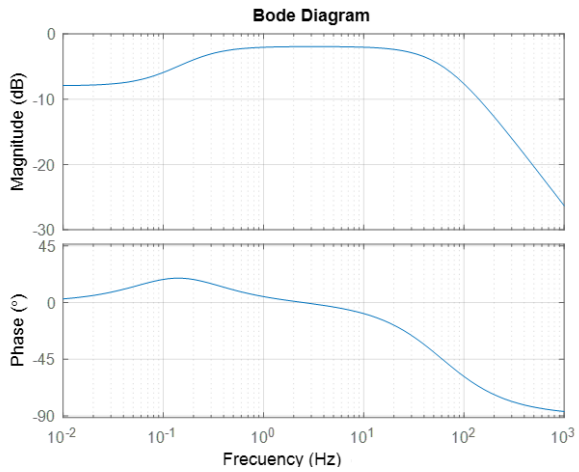

Fig. 7 Frequency response for the otolith model

Table 2 shows the specific parameters of the rotational motion model for the semicircular system, and the frequency response of the rotational sensation transfer function for the semicircular channel is shown in Figure 8.

Table 2

Parameters specific to rotational motion for the semicircular system [24]

	Roll (x)	**Pitch (y)**	**Yaw (z)**
$\boldsymbol{k_{ot}}$	0.4	0.4	0.4
$\boldsymbol{\tau_1}$ $[s]$	5	5	5
$\boldsymbol{\tau_2}$ $[s]$	0.016	0.016	0.016
$\boldsymbol{\tau_L}$ $[s]$	10	10	10
$\boldsymbol{A_0}$ $[s^{-1}]$	$1/\tau_L$	$1/\tau_L$	$1/\tau_L$
$\boldsymbol{B_0}$ $[s^{-1}]$	$1/\tau_1$	$1/\tau_1$	$1/\tau_1$
$\boldsymbol{B_1}$ $[s^{-1}]$	$1/\tau_2$	$1/\tau_2$	$1/\tau_2$
$\boldsymbol{k_0}$	$k_{ot}\tau_1\tau_2/\tau_L$	$k_{ot}\tau_1\tau_2/\tau_L$	$k_{ot}\tau_1\tau_2/\tau_L$
$\boldsymbol{\delta TH}$ $[deg/s]$	0.17	0.17	0.28

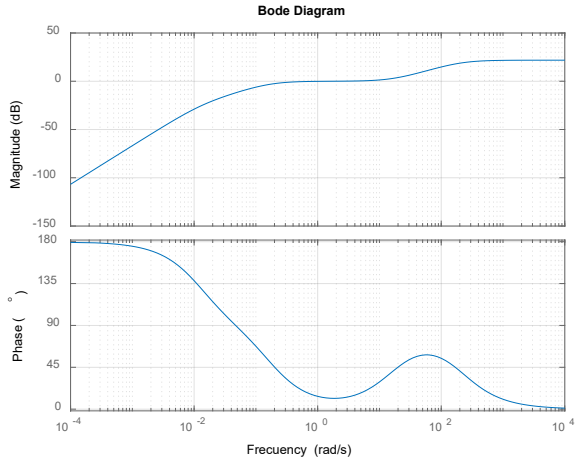

Fig. 8 Frequency response for the semicircular system

The results of the OWF and the modified OFW based on genetic algorithms are then presented. Graphical representations of the flight information and a comparison between the results of the two filters for linear acceleration, roll and pitch motion for different flight phases are presented. The results are presented for short time sequences of a cruise flight phase. Figure 8 shows the parameters describing the flight segment (latitude - longitude, altitude, heading, Mach number) for the cruise flight phase sequence for one flight scenario.

In Figures 10, 11 and 12 it can be seen that the signal recorded by the modified OWF based on the genetic algorithm (GA) provides a correction of the signal shape for the states recorded by the original algorithm with a visible improvement for the roll angle.

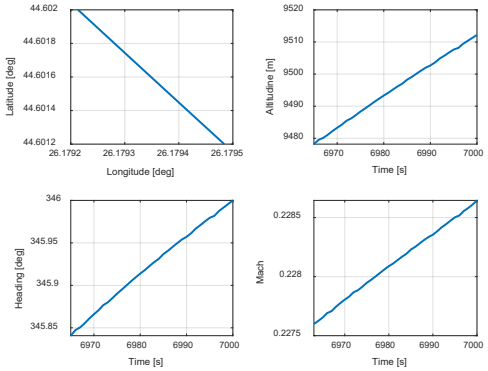

Fig. 9 Flight scenario - flight parameters cruise sequence

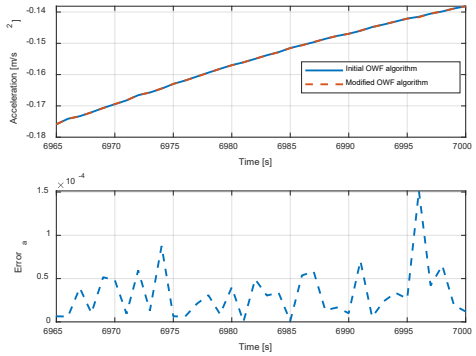

Fig. 10 Acceleration – Comparison between initial OWF and modified OWF - GA

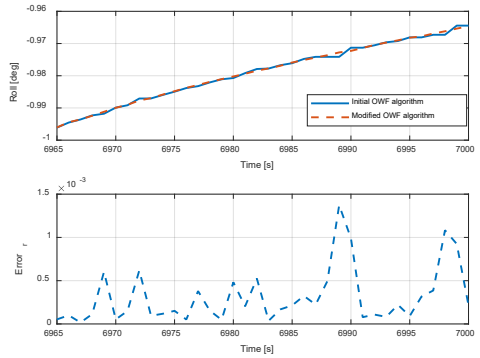

Fig. 11 Roll angle - Comparison between initial OWF and modified OWF – GA

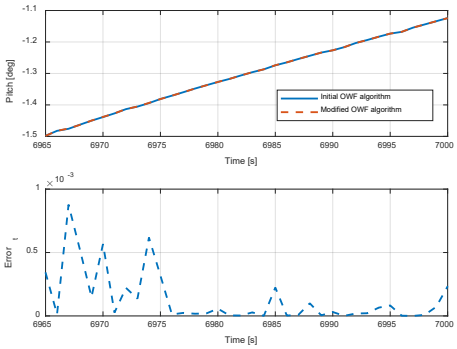

Fig. 12 Pitch angle - Comparison between initial OWF and modified OWF – GA

The results show the effect on the fidelity of the motion indices. From the graphical representations it can be seen that for pitch and roll motion the models show almost identical continuity of signal shape, the output signal is able to track the modified wash filter reference signal with a significantly higher degree of correlation, the average error recorded is in the order of $\mathbf{10^{-4}}$.

The modified optimal wash filter algorithm generates better motion with a more realistic feel in a more efficient way by reducing platform displacement. As a result, the simulator can efficiently use the extra space for other possible motions.

6. Conclusion

The motion algorithm is responsible for transforming the acceleration and angular velocity of a simulated vehicle in order to reproduce high fidelity motion within the

physical limits of the simulator. The OWF was designed based on the LQR method which takes into account the vestibular system and the motion of the simulator to reduce the human perception error between the simulator and the real aircraft in the most efficient way. Due to other physical limitations of the ABB IRB 7600-500 serial robot system, a constraint was applied to the translation and rotation channels. At the same time, scaling was applied to the state vector signals ($\boldsymbol{u_{A/C}}$) used as input to the algorithm model a scaling was applied to change the signal amplitude uniformly across all frequencies. A third order polynomial was used and implemented in the general scheme of the OWF algorithm. The scaling and limiting units play an important role in keeping the motions within the physical limits of the flight simulator, and are used in conjunction with the OWF to reduce the magnitude of the translational and rotational motion signals uniformly across all frequencies in the algorithm, so as to mitigate the effects of workspace limitations in reproducing the simulator motion and to improve the realism of the motion feel.

To improve the OWF, a new strategy based on evolutionary algorithms was proposed. The main objective was to regenerate a signal that could closely track the reference signal, avoid false motion cues and improve its shape. A number of criteria were considered in the cost function of the GA, such as the error of human perception, the correlation coefficient and the limiting function.

The results show the superiority of the proposed OWF based on genetic algorithm due to its better performance, improved human perception, increased shape tracking factor and reduced displacement. Since a balance between human perception error and shape tracking has been achieved, the proposed OWF algorithm generates better motion and can provide more realistic feeling to the pilot in the simulator more efficiently. The results showed that the algorithm is reliable, robust and efficient in this application for the ABB IRB 7600-500 serial robot motion platform-based flight simulator.

The advantage of this study is that the proposed algorithm can be used as a tool for any other type of simulator with different physical constraints, or for the same simulator in different physical configurations, without requiring much effort to tune the specific parameters of the motion algorithm.

REFERENCES

[1]. *Peter R. Grant, Lloyd Reid*, "Motion washout filter tuning: Rules and requirements," Journal Aircraft, vol. 34, no. 2, pp. 145-151, 1997.

[2]. *Raphael Sivan, Jehuda Ish-Shalom, Jen-K Huang*, "An optimal control approach to the design of moving flight simulators," IEEE Transactions on Systems, Man and Cybernetics, vol. 12, no. 6, pp. 818-827, 1982.

[3]. *Russell V. Parrish, James E. Dieudonne, Roland L. Bowles, Dennis J Martin Jr.*, "Coordinated adaptive washout for motion simulators," Journal of Aircraft, vol. 12, no. 1, pp. 44-50, 1975.

[4]. *Chau Chung Song, Der-Cherng Liaw, Wen Ching Chung*, "Washout-filter based bifurcation control of longitudinal flight dynamics," IEEE Region 10 Conference on Computers, Communications, Control and Power, pp. 1646-1649, 2002.

[5]. *Su-Chiun Wang, Li-Chen Fu*, "Predictive washout filter design for VR-based motion simulator," IEEE International Conference on Systems, Man and Cybernetics, pp. 6291-6295, 2004.

[6]. *Houshyar Asadi, Shady Mohamed, Chee Peng Lim, Saeid Nahavandi*, "Robust optimal motion cueing algorithm based on the linear quadratic regulator method and a genetic algorithm," IEEE Transactions on Systems, Man, and Cybernetics: Systems, pp. 1-17, 2016.

[7]. *Sue-Huei Chen, Li-Chen Fu*, "An optimal washout filter design with fuzzy compensation for a motion platform," 18th IFAC World Congress, IFAC Proceedings, vol. 44, no. 1, pp. 8433-8438, 2011.

[8]. *Mohammad Reza Gharib*, "Comparison of robust optimal QFT controller with TFC and MFC controller in a multi-input multioutput system," Reports in Mechanical Engineering, vol. 1, no. 1, pp. 151-161, 2020.

[9]. *Chin-I Huang, Li-Chen Fu*, "Human Vestibular Based (HVB) Senseless maneuver optimal washout filter design for VR-based motion simulator," IEEE International Conference on Systems, Man and Cybernetics, pp. 4451-4458, 2006.

[10]. *Xiang-Tong Kong, Yuan-Chang Zhu, Yan-Qiang Di, Hao-Hao Cui,* "Methods to determine optimal washout position for single and multioccupant motion simulator," Cybernetics and Information Technologies, vol. 16, no. 1, pp. 173-187, 2016.

[11]. *Hichem Arioui, Lamri Nehaoua, Ali Amouri*, "Classic and adaptive washout comparison for a low cost driving simulator," Proceedings of the 2005 IEEE International Symposium on Mediterrean Conference on Control and Automation, pp. 586-591, 2005.

[12]. *Sue-Huei Chen, Li-Chen Fu*, "An optimal washout filter design for a motion platform with senseless and angular scaling maneuvers," IFAC Proceedings, vol. 44, no. 1, pp. 8433-8438, 2010.

[13]. *Xun-Li Wang, Li L., Zhang W. H.*, "Research on fuzzy adaptive washout algorithm of train driving simulator," Tiedao Xuebao/Journal of the China Railway Society , vol. 32, no. 2, pp. 31-36, 2010.

[14]. *Yu Yang, Qi-tao Huang, Jun-wei Han,* "Adaptive washout algorithm based on the parallel mechanism motion range," Xi Tong Gong Cheng Yu Dian Zi Ji Shu/Systems Engineering and Electronics, vol. 32, no. 12, pp. 2716-2720, 2010.

[15]. *Majid Moavenian, Mohammadreza Gharib, Armin Daneshvar, Salman Alimardani*, "Control of human hand considering uncertainties," IEEE International Conference on Advanced Mechatronic Systems, pp. 17-22, 2011.

[16]. *Kyoung Dal Kim, Moon Sik Kim, Young Geun Moon, Min Cheol Lee*, "Application of vehicle driving simulator using new washout algorithm and robust control," SICE-ICASE International Joint Conference, pp. 2121-2126, 2006.

[17]. *Mohammad Reza Salehi Kolahi, Mohammad Reza Gharib, Ali Koochi*, "Design of a robust control scheme for path tracking and beyond pull-in stabilization of micro/nano-positioners in the presence of Casimir force and external disturbances," Archive of Applied Mechanics, vol. 91, no. 10, pp. 4191-4204, 2021.

[18]. *Robert J. Telban, Frank M. Cardullo,* "Motion cueing algorithm development: Human-centered linear and nonlinear approaches," NASA Langley Research, Techical Report CR-2005-213747, Hampton, VA, USA, 2005.

[19]. *Anthony Van Egmond, Johannes Groen, Leonard B.W. Jongkees*, "The Mechanics of the Semicircular Canal," Journal of Physiology, vol. 110, pp. 1-17, 1949.

[20]. *Alina-Ioana Chira, Marian Ciprian Bîlu, Răzvan Ionuț Bălașa, Cătălin Iordache*, "Enhancing Realism in Robotic Flight Simulators: a case study on the implementation analysis of a washout filter," in 34th DAAAM International Symposium on Intelligent Manufacturing and Automation, Vienna, 2023.

[21]. *Peter J. Fleming, Robert C. Pyrshouse*, "Evolutionary algorithms in control systems engineering: A survey," in Control Engineering Practice, 2002.

[22]. *Xin-She Yang,* "Chapter 5 Genetic Algorithms," in Nature-Inspired Optimization Algorithms, 2014.

*[23]. Fauzi Mohd Johar, Farah Ayuni Azmin, Mohamad Kadim Suaidi, Abdul Samad Shibghatullah, Badrul Hisham Ahmad, Siti Nadzirah Salleh, Mohamad Zoinol Abidin Abdul Aziz, Mahfuzah Md. Shukor, "*A review of genetic algorithms and parallel genetic algorithms on graphics processing unit (GPU)," in Proc. IEEE Int. Conf. Control Syst. Comput. Eng. (ICCSCE), pp.264-269 Penang, 2013.

[24]. *Alina-Ioana Chira*, "Contributions to motion cueing algorithms for flight simulators," PhD Thesis, National University of Science and Technology POLITEHNICA Bucharest, 2024.